Inelastic Diffraction Scattering*

E. Rost† and N. Austern
University of Pittsburgh, Pittsburgh, Pennsylvania
(Received July 12, 1960)

The method of distorted waves Born approximation is shown to be equivalent to the first-order adiabatic method for the calculation of inelastic scattering. The flexibility of the distorted waves method is indicated and tested by numerical calculation for a simplified model. The calculations treat the inelastic scattering of alpha particles from strongly absorbing nuclei, and are directly comparable to the adiabatic calculations considered by Blair in Fraunhofer approximation. Good agreement is found at forward angles. Coulomb wave functions are used, and the energy difference between initial and final states is taken into account. Comparison is made to a few representative experiments and good agreement is found.

I. INTRODUCTION

MANY strong inelastic scattering transitions of nuclei obviously are surface direct reactions, on the evidence of their rapidly-varying oscillatory angular distributions.[1] Such rapid variation with angle indicates the importance of large impact parameters. In addition the oscillations of the angular distributions often are very regular, and this seems to agree with some of the results for surface reactions, as found in plane wave Born approximation.[2] Further evidence that the strong inelastic scattering transitions take place at the nuclear surface is found in the property that they mostly seem to involve collective excitations,[3] probably of vibrations and rotations of the surface. It should be possible to understand reactions which have such well-defined properties, and to understand their relationships with other sorts of direct reactions.

Unfortunately, the clearest oscillatory angular distributions generally appear in experiments with projectiles which are strongly absorbed, such as alpha particles. Although inelastic scattering of such projectiles almost certainly occurs at the nuclear surface, the plane-wave Born approximation calculation also certainly is not applicable. Distorted wave Born approximation (DWB) and the adiabatic method instead are applied to understand these reactions.

The DWB method[4] is the most widely accepted procedure for treating direct reactions, and gives a rather unified view of them. In this method the initial state of a nucleus is described by v_i, say, and the final state by v_f, and the transition amplitude for inelastic scattering from state i to state f is given by

$$T_{fi}=\langle v_f\chi_f^{(-)}\,|\,V\,|\,v_i\chi_i^{(+)}\rangle. \tag{1}$$

The cross section is

$$(d\sigma_{fi}/d\Omega)=(M/2\pi\hbar^2)^2(k_f/k_i)\textstyle\sum_{\rm av}|\,T_{fi}\,|^2. \tag{2}$$

Here $\chi_i^{(+)}$ and $\chi_f^{(-)}$ are the exact wave functions for the motion of the projectile with respect to the nucleus; they are eigenstates of the optical model interaction between the projectile and the target. Thus

$$[-(\hbar^2/2M)\nabla^2+U]\chi_{i,f}^{(\pm)}=E_{i,f}\chi_{i,f}^{(\pm)}, \tag{3}$$

where U is the optical interaction. The potential V causes the transition, but does not influence the "distorted waves" $\chi_i^{(+)}$ and $\chi_f^{(-)}$. For excitations of the surface V is that part of the optical potential caused by deformation of the nucleus from its equilibrium shape,[2,5] while U is the equilibrium part of the optical potential. Slight generalizations of these equations are used when other direct reactions are treated.

Accurate DWB calculations are laborious. Simplified considerations[6] suggested that for the more strongly absorbed projectiles such calculations would not even agree with experiment, that oscillatory angular distributions would not be obtained. This difficulty led Blair[7] to stress the adiabatic method,[8] already introduced by Drozdov and Inopin[9] to study inelastic scattering.

In the adiabatic method T_{fi} is calculated in two steps,

* Work done at Sarah Mellon Scaife Radiation Laboratory and supported by the joint program of the Office of Naval Research and the U. S. Atomic Energy Commission.

† National Science Foundation Cooperative Graduate Fellow.

[1] For example: P. C. Gugelot and M. Rickey, Phys. Rev. **101**, 1613 (1956); A. I. Yavin and G. W. Farwell, Nuclear Phys. **12**, 1 (1959); G. B. Shook, Phys. Rev. **114**, 310 (1959).

[2] N. Austern, S. T. Butler, and H. McManus, Phys. Rev. **92**, 350 (1953); D. M. Brink, Proc. Phys. Soc. (London) **A68**, 994 (1955); S. Hayakawa and S. Yoshida, Progr. Theoret. Phys. (Kyoto) **14**, 1 (1955); Proc. Phys. Soc. (London) **A68**, 656 (1955).

[3] B. L. Cohen, Phys. Rev. **116**, 426 (1959); also see J. S. Blair, reference 7.

[4] W. Tobocman, Phys. Rev. **115**, 98 (1959); M. Gell-Mann and M. L. Goldberger, Phys. Rev. **91**, 398 (1953); C. A. Levinson and M. K. Banerjee, Ann. Phys. **2**, 471 (1957); A review is given by N. Austern, *Fast Neutron Physics*, edited by J. B. Marion and J. L. Fowler (Interscience Publishers, New York, 1960), Vol. II, Chap. V.

[5] D. M. Chase, L. Wilets, and A. R. Edmonds, Phys. Rev. **110**, 1080 (1958).

[6] S. T. Butler, N. Austern, and C. Pearson, Phys. Rev. **112**, 1227 (1958).

[7] J. S. Blair, Phys. Rev. **115**, 928 (1959).

[8] D. M. Chase, Phys. Rev. **104**, 838 (1956).

[9] S. I. Drozdov, J. Exptl. Theoret. Phys. (U.S.S.R.) **28**, 734 and 736 (1955); [translation: Soviet Phys.-JETP **1**, 591 and 588 (1955)]; S. I. Drozdov, J. Exptl. Theoret. Phys. (U.S.S.R.) **30**, 786 (1956) [translation: Soviet Phys.-JETP **3**, 759 (1956)]; S. I. Drozdov. J. Exptl. Theoret. Phys. (U.S.S.R.) **34**, 1288 (1958) [translation: Soviet Phys.-JETP **7**, 889 (1958)]; S. I. Drozdov, J. Exptl. Theoret. Phys. (U.S.S.R.) **36**, 1875 (1959) [translation: Soviet Phys.-JETP **9**, 1335 (1959)]; E. V. Inopin, J. Exptl. Theoret. Phys. (U.S.S.R.) **31**, 901 (1956) [translation: Soviet Phys.-JETP **4**, 764 (1957)].

a division being made on the basis that the wave function of the target nucleus, initially $v_i(\alpha)$, responds slowly to the perturbation V. First the elastic scattering amplitude $f(\theta,\phi,\alpha)$ is computed for each fixed value of the internal variable α, i.e., for each of the variety of possible nuclear shapes. This gives

$$f(\theta,\phi,\alpha)=(M/2\pi\hbar^2)\int d^3r\,\phi_f^*\{U(r)+V(\mathbf{r},\alpha)\}\psi_i^{(+)}, \quad (4)$$

where ϕ_f is a plane wave, and $\psi_i^{(+)}(\mathbf{r},\alpha)$ is the scattering eigenstate of $\{U+V\}$. In the next step an integral over α is computed, and

$$\begin{aligned} T_{fi}&=(2\pi\hbar^2/M)\langle v_f|\,f(\theta,\phi,\alpha)\,|v_i\rangle \\ &=\langle v_f\phi_f|\,U+V(\mathbf{r},\alpha)\,|v_i\psi_i^{(+)}\rangle. \end{aligned} \quad (5)$$

Evidently the exact evaluation of Eqs. (4) and (5) is even more difficult than the corresponding DWB calculations, because the eigenfunction $\psi_i^{(+)}(\mathbf{r},\alpha)$ is difficult to compute, and must be computed for each α. Closed form expressions for $f(\phi,\theta,\alpha)$ have been obtained for an important limiting case, however, for the small-angle scattering of particles of small wavelength by nuclei with small deformations.[7] Most (α,α') results are for cases not too far from this "Fraunhofer" limit, so it is helpful that simple approximate formulas can be obtained. Encouraging agreement with experiment is found. Unfortunately, it does not seem practical to use the adiabatic method for much more accurate calculations than these.

Actually, in the limit of small deformations the adiabatic method is formally identical with the DWB method. Thus, let

$$\psi_i^{(+)}=\chi_i^{(+)}+\Delta\psi,$$

and let it be understood that in $\Delta\psi$ only the terms first order in V shall be carried. Then because v_f and v_i are orthogonal, Eq. (5) becomes to first order

$$T_{fi}=\langle v_f\phi_f|\,V\,|v_i\chi_i^{(+)}\rangle+\langle v_f\phi_f|\,U\,|v_i\Delta\psi\rangle. \quad (6)$$

The difficulties of the adiabatic method are concerned with the calculation of $\Delta\psi$. The DWB method instead eliminates consideration of $\Delta\psi$ by an *exact* transformation[10] which introduces the distorted final wave $\chi_f^{(-)}$. The transformation converts the expression of Eq. (6) to identically that of Eq. (1).

It is helpful that a return to the DWB method for alpha-particle inelastic scattering has become possible. This restores a unified treatment of the direct reaction theories. It becomes clear that the angular distributions of (α,α') reactions must be almost independent of the mode of excitation, so that collective modes and single particle modes must differ primarily in their absolute cross sections. The inherent similarity between (α,α') and all other surface reactions, such as (α,p) also is clarified. One further advantage is that it is easier to use accurate wave functions in the DWB method than in the adiabatic method, so several physical phenomena omitted before can now be studied. Thus, DWB is more general than the adiabatic method.

If generality is not required the adiabatic method offers important advantages for the particular problem of inelastic scattering, and gives simple closed form expressions for the region of small scattering angles. For this region it predicts absolute cross sections, and shows the relationship between the elastic and inelastic scattering cross sections. In principle these results all should be available from DWB, but not so easily.

The earlier suggestions of failure of the DWB method were indicated by a "semiclassical" model,[6] based upon the use of WKB wave functions, and exhibiting results resembling those of physical optics. For surface reactions the model predicts that oscillatory angular distributions occur if there is interference between outgoing particle beams which have traversed widely separated parts of the surface. Such beams have different path lengths, so have different phases. The model limits the "active" regions on the surface, those which the particle beams may traverse, by relating these regions to the quantized angular momentum transferred in the reaction. Disagreement with experiment then is demonstrated by observing that the "active" regions on the surface generally are so placed that strong absorption of the particle beams by the nucleus limits one beam much more than the other, so suppresses their interference. Oscillations in the cross section thereby are suppressed. Fortunately, although the semiclassical model was derived from the quantum mechanical DWB expression, the derivation breaks down if distortion is very strong. The derivation selects "active" regions in the DWB integral by a stationary phase technique, this technique selecting the important parts of the integrand. Now, the basis of selection ought to become more stringent as the integrand becomes complicated by the enhancement of distortion, if the semiclassical model is to retain its accuracy. However, the regions of stationary phase become dominant in the integral only in the limit *both* of large momentum transfer and large angular momentum transfer. In the applications of interest the *angular* momentum transfer never is large enough to select "active" regions in the presence of strong distortion. Thus the semiclassical model gives false indications of the nature of DWB results.

The purpose of the present paper is to exploit the equivalence between the adiabatic and DWB methods. In Secs. II and III an abbreviated sort of distorted waves calculation is formulated, and detailed comparisons with the Fraunhofer calculations of Blair are made. The consequences of changing the physical assumptions are investigated, and are seen to be important in many cases. The cross sections are also studied at large angles, where the Fraunhofer method breaks down.

Section II describes in detail the assumptions used to obtain wave functions for the DWB computation, and

[10] This is discussed by Gell-Mann and Goldberger, reference 4.

the nature of the computation. The results of computation are given in Sec. III, along with discussion of their sensitivity to the assumptions. Comparison with experiment is given in Sec. IV.

II. DESCRIPTION OF THE CALCULATION

(a) Cross Section Formula for $L=2$ Excitation

In this section we consider in detail the calculation in distorted wave Born approximation of the transition amplitude for inelastic scattering. Equations (1) and (2) already present a formal statement of the method and indicate how the cross section is computed. These expressions now will be spelled out more fully, and the approximations under which numerical calculations are made will be described.

Angular distributions computed by the distorted waves method are notably insensitive to the nature of the nuclear excitation they represent. Rotational excitation, vibrational excitation, single-particle excitation, all give much the same angular distribution. Glendenning[11] has particularly emphasized this result for the case of surface reactions. For such reactions the expression for the cross section splits exactly into two factors: One factor depends on the model for the reaction, carries the selection rules, and determines the total cross section; the other factor involves the distorted wave functions $\chi_i^{(+)}$ and $\chi_f^{(-)}$ and determines the angular distribution. Because of this convenient factoring it is necessary to conduct detailed computations only for any one reaction model; then the cross section for any other model is obtained by multiplication by a suitable constant. Such multiplicative constants already appear in the papers of Blair,[7] of Glendenning,[11] and of Goldfarb and Johnson.[12] The present discussion will emphasize the convenient special case of the excitation of a permanently deformed even-even nucleus from the $J=0$ ground state to the first $J=2$ state. This case will be treated in detail, in order to give meaning to the discussion of normalization of the cross section at the end of this section.

In T_{fi} in Eq. (1) the interaction V simply is the deformed part of the total optical potential. It is obtained to first order by differentiating the optical potential with respect to the deformation parameter of the surface,[5] on the assumption that the strength of the potential depends only on the distance from the surface, $[r-R(\theta')]$. Here R is the effective nuclear radius, given in terms of the coordinate angles (θ',ϕ') with respect to the body-fixed principal axes of the nucleus. This radius is

$$R=R_0[1+\beta Y_2^0(\theta')], \tag{7}$$

where β is the usual deformation parameter. Then the first-order term of the optical potential is found to be

$$V(r,\theta')=\beta R_0 Y_2^0(\theta')(dU/dr). \tag{8}$$

[11] N. K. Glendenning, Phys. Rev. **114**, 1297 (1959).
[12] L. J. B. Goldfarb and R. G. Johnson (to be published).

The optical wave functions $\chi_i^{(+)}$ and $\chi_f^{(-)}$ are written in space-fixed coordinate axes. It is convenient to take the direction of the incident beam as the polar axis of the space-fixed system. The initial wave function and the complex conjugate of the final wave function may then be written in partial wave expansion as

$$\chi_i^{(+)}(\mathbf{k}_i,\mathbf{r})=[(4\pi)^{\frac{1}{2}}/k_i r]\times\sum_{l=0}^{\infty} i^l(2l+1)^{\frac{1}{2}}e^{i\sigma_l}f_l(k_i,r)Y_l^0(\Omega), \tag{9a}$$

$$\chi_f^{(-)*}(\mathbf{k}_f,\mathbf{r})=(4\pi/k_f r)\sum_{l'=0}^{\infty}\sum_{m'=-l'}^{l'} i^{-l'}e^{i\sigma_{l'}}f_{l'}(k_f,r)\times Y_{l'}^{m'}(\Theta,0)Y_{l'}^{m'*}(\Omega). \tag{9b}$$

In Eqs. (9) the symbols $\mathbf{k}_i$ and $\mathbf{k}_f$ are the incident and outgoing propagation constants, the corresponding incident and outgoing energies being

$$E_i=\hbar^2k_i^2/2M, \quad E_f=\hbar^2k_f^2/2M,$$

in center-of-mass coordinates,[13] with M the reduced mass of the system. The angle between $\mathbf{k}_i$ and $\mathbf{k}_f$ is Θ, the scattering angle. The wave functions are arranged to meet the asymptotic boundary conditions

$$\chi^{(+)} \underset{r\to\infty}{\longrightarrow} e^{i(\mathbf{k}\cdot\mathbf{r})}+\text{outgoing scattered waves},$$

$$\chi^{(-)} \underset{r\to\infty}{\longrightarrow} e^{i(\mathbf{k}\cdot\mathbf{r})}+\text{incoming scattered waves}.$$

Equation (9b) is obtained from the usual time-reversal equation

$$\chi^{(-)*}(\mathbf{k},\mathbf{r})=\chi^{(+)}(-\mathbf{k},\mathbf{r}).$$

It is especially seen from the discussion of Breit and Bethe[14] that this equation holds without modification even though the optical potential U is made complex.[15] The same result is found by Biedenharn.[16]

Both the radial functions $f_l(k_i,r)$ and $f_l(k_f,r)$ satisfy the differential equation

$$[-d^2/dr^2+l(l+1)r^{-2}+(2M/\hbar^2)U(r)+(2kn/r)-k^2]f_l(k,r)=0. \tag{10}$$

The Coulomb parameter n is

$$n=ZZ'Me^2/\hbar^2k,$$

where Z is the charge number of the target and Z' that of the projectile. The boundary conditions satisfied by f_l are that it vanish at $r=0$, and that asymptotically as $r\to\infty$

$$f_l\to(i/2)(H_l^*-\eta_l H_l). \tag{11}$$

[13] The distorted waves method achieves an interesting improvement on the adiabatic method in that it is not necessary for E_f to equal E_i.
[14] G. Breit and H. A. Bethe, Phys. Rev. **93**, 888 (1954).
[15] It may be helpful to observe that the basic orthogonality integral, $\int_0^\infty f_l(k,r)f_l(k',r)dr=\frac{1}{2}\pi\delta(k-k')$, does not involve the operation of complex conjugation.
[16] L. C. Biedenharn, Nuclear Phys. **10**, 620 (1959).

The quantity η_l is the diagonal S-matrix element for the channel in question, as defined by Blatt and Weisskopf.[17] It assumes the value $\eta_l=1$ if there is no interaction, and otherwise is given in terms of the phase shift as $\eta_l=\exp(2i\delta_l)$. Generally $|\eta_l|<1$ because U is complex. The function $H_l(kr)$ is that defined by Hull and Breit[18] to be the Coulomb analog of $ikrh_l^{(1)}(kr)$, where $h_l^{(1)}$ is the outgoing spherical Hankel function.[19] In terms of the regular and irregular radial Coulomb functions of Breit,

$$H_l(kr)=G_l(kr)+iF_l(kr),$$

where asymptotically

$$F_l\rightarrow\sin\theta_l,$$
$$G_l\rightarrow\cos\theta_l,$$

and

$$\theta_l=kr-n\ln(2kr)-(l\pi/2)+\sigma_l,$$
$$\sigma_l=\arg\Gamma(l+1+in).$$

The method for computing the Coulomb wave functions is discussed in the Appendix.

The only remaining wave functions which must be known in order to compute T_{fi} are the nuclear wave functions v_i and v_f. These express the orientation of the ellipsoidal nucleus with respect to a space-fixed coordinate system. In the ground-state band the ellipsoid has no spin about its symmetry axis, so v_i and v_f are just spherical harmonics giving the orientation of the axis. Thus

$$\begin{aligned} v_i&=Y_0{}^0(\theta_1,\theta_2),\\ v_f&=Y_2{}^M(\theta_1,\theta_2),\end{aligned}\tag{12}$$

where (θ_1,θ_2) are the orientation angles with respect to the space-fixed frame.

To compute the transition amplitude, it is convenient to re-express the interaction of Eq. (8) in terms of the space-fixed coordinates, in place of the body-fixed coordinates. Through use of the addition theorem for spherical harmonics it follows that

$$V(r,\theta')=\beta R_0(dU/dr)(4\pi/5)^{\frac{1}{2}}\textstyle\sum_\mu Y_2{}^{\mu*}(\Omega)Y_2{}^\mu(\theta_1,\theta_2).\tag{13}$$

This expression and the wave functions are substituted into Eq. (1), giving

$$\begin{aligned}T_{fi}=\beta R_0(4\pi/5)^{\frac{1}{2}}&\textstyle\sum_\mu\langle v_f|\,Y_2{}^\mu(\theta_1,\theta_2)\,|v_i\rangle\\ &\times\langle\chi_f{}^{(-)}|\,Y_2{}^{\mu*}(\Omega)(dU/dr)\,|\chi_i{}^{(+)}\rangle.\end{aligned}\tag{14}$$

Equation (14) displays the factoring of the transition amplitude, mentioned earlier. Any other reaction model for quadrupole excitation must involve the same spherical harmonics as do the two factors of Eq. (14). Changing the model tends only to change the first factor and thus only to change a normalization coefficient. The second factor of Eq. (14) involves an integration over r. This integration does influence the angular distribution and may be somewhat model-dependent. Nevertheless for all surface reactions, as the present case is seen to approximate, the integration emphasizes only a limited range of r, and therefore a single characteristic angular distribution is obtained. Expressions corresponding to Eq. (14) are obtained for other cases, and for other values of angular momentum transfer, by suitably changing the indicated spherical harmonics in Eq. (14), and by changing the normalization.[7,11,12]

The result of performing the various integrations in Eq. (14) is found to be

$$\begin{aligned}T_{fi}{}^M=4\pi\beta R_0k_i{}^{-1}k_f{}^{-1}&\textstyle\sum_{l,l'}i^{l-l'}(2l'+1)^{\frac{1}{2}}e^{i(\sigma_l+\sigma_{l'})}\\ &\times I_{ll'}Y_{l'}{}^{-M}(\Theta,0)C_{000}{}^{l'2l}C_{-MM0}{}^{l'2l},\end{aligned}\tag{15}$$

$$I_{ll'}\equiv\int_0^\infty(dU/dr)f_lf_{l'}dr.\tag{16}$$

The notation used for Clebsch-Gordan coefficients is

$$C_{m_1m_2M}{}^{j_1j_2J}=\langle j_1j_2m_1m_2|\,JM\rangle.$$

To obtain the differential cross section, $T_{fi}{}^M$ of Eq. (15) is squared and summed over values of M, the final state spin projection. No average over initial states need be performed, as the ground state has spin zero, and in the absence of spin-orbit coupling the projectile spin cancels out. Then

$$\begin{aligned}(d\sigma_{fi}/d\Omega)=(\beta^2R_0{}^2/E_iE_f)(k_f/k_i)&\\ \times\textstyle\sum_{M=0,1,2}\epsilon_M|\sum_{l,l'}i^{l-l'}(2l'+1)^{\frac{1}{2}}e^{i(\sigma_l+\sigma_{l'})}&\\ \times I_{ll'}Y_{l'}{}^M(\Theta,0)C_{000}{}^{l'2l}C_{-MM0}{}^{l'2l}|^2,&\\ \epsilon_M=2-\delta_{M,0}.&\end{aligned}\tag{17}$$

Numerical evaluation of Eq. (17) is done most easily if the invariant formalism[20] for summing over M is not used, as that procedure eventually leads to a complicated multiple sum. Instead, the double sum over l, l' is best performed numerically for each value of M, and this result squared and summed over M. The Clebsch-Gordan coefficients limit l in Eq. (17) to the small set of values $l=l'$, or $l'\pm2$. Using suitable approximations for $I_{ll'}$, to be discussed below, Eq. (17) has been programmed for the University of Pittsburgh IBM 650 computer. The running time for a typical case is ten minutes.

(b) Approximation of Radial Integrals

If (dU/dr) were a delta function the difficult radial integrals $I_{ll'}$ of Eq. (16) would be easy to compute. The result would be

$$I_{ll'}=V_0f_l(\rho_i)f_{l'}(\rho_f),\tag{18}$$

[17] J. M. Blatt and V. F. Weisskopf, *Theoretical Nuclear Physics* (John Wiley & Sons, Inc., New York, 1952), Chap. VIII.

[18] M. H. Hull, Jr., and G. Breit, *Encyclopedia of Physics*, edited by S. Flügge (Springer-Verlag, Berlin, 1959), Vol. 41, Part 1, p. 410.

[19] L. I. Schiff, *Quantum Mechanics* (McGraw-Hill Book Company, New York, 1955).

[20] J. M. Blatt and L. C. Biedenharn, Revs. Modern Phys. **24**, 258 (1952).

where $\rho_{i,f}\equiv k_{i,f}R_0$ denotes the argument of f_l at the nuclear surface. (The f_l are functions of the product kr if $r\gtrsim R_0$.) Analysis of the actual radial integrals is given in Sec. II(c), below, and in the Appendix. It will be seen that replacing the integral by a constant multiple of the value of the integrand at some "surface" radius is approximately correct within the range of values of l' which contribute strongly to the cross section. Also, it will be seen that at the radius which is important the radial wave functions already are accurately asymptotic. These approximations are suitable for testing the distorted waves method and for showing its more important improvements upon the Fraunhofer approximation[7] to the adiabatic method. Upon introducing the approximations in Eq. (17) the result becomes

$$(d\sigma_{fi}/d\Omega)=\beta^2R_0^2(V_0^2/E_iE_f)(k_f/k_i)\times\sum_{M=0,1,2}\epsilon_M\Big|\sum_{l,l'}i^{l-l'}(2l'+1)^{\frac{1}{2}}e^{i(\sigma_l+\sigma_{l'})}f_l(\rho_i)\times f_{l'}(\rho_f)Y_{l'}{}^M(\Theta,0)C_{000}{}^{l'2l}C_{-MM0}{}^{l'2l}\Big|^2. \quad (19)$$

It will be seen in Sec. II(c) that the parameter V_0 varies with energy, such that (V_0^2/E_iE_f) tends to be constant. It is Eq. (19) which was programmed for the computer.

The radial functions f_l need to be evaluated at the nuclear surface, where the optical potential already is very weak, so that the asymptotic form of $f_l(\rho)$ given in Eq. (11) is valid. Hence, the problem of obtaining the radial functions reduces to the evaluation of the diagonal S-matrix elements

$$\eta_l=c_le^{i\xi_l}, \quad (20)$$

where c_l and ξ_l are the modulus and phase of the complex quantity η_l. This can be accomplished by integrating the differential equation, Eq. (10), from $r=0$ to $r=R_0$ and matching the solution to the asymptotic form given by Eq. (11) at $r=R_0$, thus determining η_l. This procedure was used for a few cases where optical potentials were available.[21]

For convenience in testing the distorted waves theory it was desirable to circumvent the difficult optical-model calculations, and to assume various simple analytic expressions for the η_l. One simple expression which is valid in the limit of short wavelength and strong absorption is the sharp-cutoff model[22] of Bethe and Placzcek. The sharp-cutoff model assumes $\eta_l=0$ for $l<\rho$, corresponding to complete absorption; and assumes $\eta_l=1$ for $l>\rho$, corresponding to no interaction. A somewhat better assumption has been used by McIntyre, Wang, and Becker[23] who write

$$c_l=\{1+\exp[(\rho-l)/\Delta l]\}^{-1}, \quad (21a)$$

$$\xi_l=\xi^{(0)}\{1+\exp[(l-\rho)/\Delta l]\}^{-1}. \quad (21b)$$

The quantities $\xi^{(0)}$ and Δl are to be regarded as free parameters which are adjusted to fit the elastic scattering. If necessary, Δl and ρ need not be the same in (21a) and (21b) and ρ need not be equal to kR_0; however, we have not used this freedom. By employing the "smoothing" procedure of Eq. (21), McIntyre *et al.* are able to obtain excellent fits to several elastic scattering experiments involving alpha particles. However, it must be emphasized that there is no theoretical justification for the functional form of Eq. (21). Another "smoothing" form is

$$\begin{aligned} c_l&=0; & \xi_l&=\xi^{(0)}; & l&<\rho-2\Delta l\\ &=\tfrac{1}{2}[1+(l-\rho)/2\Delta l]; & &=(\xi^{(0)}/2)[1-(l-\rho)/2\Delta l]; & \rho-2\Delta l&<l<\rho+2\Delta l \quad (22)\\ &=1; & &=0; & l&>\rho+2\Delta l, \end{aligned}$$

and represents linear interpolation in the modulus and phase of the S-matrix elements, over an interval of $4\Delta l$ centered at $l=\rho$. This form is somewhat simpler than the McIntyre form and consequently was used for most of the calculations to be reported. For the same value of Δl, the two "smoothing" forms have the same slope at $l=\rho$. In his analysis of the elastic scattering of 40-Mev alpha particles on Ag, McIntyre finds a reasonable fit using $\Delta l\approx 1.0$. To extrapolate this result to other cases, it seems reasonable to relate Δl to the surface thickness of the nucleus. Since optical-model calculations have shown the surface thickness to be rather constant, we set $\Delta l=1.0$ for all 40-Mev problems and modify Δl by a factor $(E/40)^{\frac{1}{3}}$ for other energies. The phase $\xi^{(0)}$ is known to be small for Ag (about 8°) and hence is safely set to zero for light elements. The effects of these assumptions are investigated in detail in Sec. III.

(c) Discussion of Radial Integrals: Normalization

The distorted waves calculation would be straightforward if a correct optical potential were used, such as that given by Igo,[24] and if (dU/dr) and the eigenfunctions f_l and $f_{l'}$ were computed consistently from the optical potential. For convenience we instead use the approximate Eq. (18) for the radial integrals. It is necessary to judge how this approximation affects the angular distributions, and what the best value of the parameter V_0 should be. It will be concluded that Eq. (18) gives an angular distribution which is reliable throughout the forward hemisphere, and that V_0 should be chosen by normalizing to the differential cross section of the adiabatic theory[7] at zero degrees scattering angle. This conclusion will be possible only for nuclei which behave rather accurately as black obstacles.

The approximate Eq. (18) assumes that the relative values of the radial integrals are the same as the relative values of the products $f_lf_{l'}$ of the radial wave functions at the interaction radius R_0. To the extent that this is

[21] We are indebted to Dr. R. Bassel for supplying us with these calculations.

[22] This model has been used extensively by Blair. See J. S. Blair, Phys. Rev. **108**, 827 (1957).

[23] J. A. McIntyre, K. H. Wang, and L. C. Becker, Phys. Rev. **117**, 1337 (1960).

[24] G. Igo, Phys. Rev. **115**, 1665 (1959).

wrong the manner in which the terms of the l, l' sum combine must be wrong, and the angular distribution must be affected. Inspection of the sum shows that only the few terms for which $l' \approx l_0$ really are large, however, and that towards forward angles these terms add in phase. Only in the backward hemisphere is there appreciable destructive interference in the sum and only there are the results at all sensitive to the assumptions. These observations are true both in the exact theory and with the approximate Eq. (18), and are the reason why Eq. (18) leads to results which are valid in the forward hemisphere.

It is easy to see that the exact $I_{ll'}$ of Eq. (16) is large only for $l' \approx l_0$, near the classical cutoff. Thus for $l' \gtrsim l_0+3$, there is very little penetration of the wave functions into the region of the potential, so $I_{ll'}$ is very small. The approximate Eq. (18) agrees with this fact, whatever value V_0 may have. For $l' \lesssim l_0-3$, the values of $I_{ll'}$ are small for another reason: The very low partial waves experience nearly complete absorption. This means that there is little back scattering of the inward propagating radial wave, that "impedance matching" is very good, that a WKB treatment must be very accurate. Thus for the low partial waves

$$f_l \approx \exp\left\{-i\int_\infty^r [k^2-2MU\hbar^{-2} -l(l+1)r^{-2}-2knr^{-1}]dr\right\}. \quad (24)$$

The integrals $I_{ll'}$ tend to average to zero if the wave functions f_l have such an oscillatory form.[25] The approximate Eq. (18) does not give very small values for the $I_{ll'}$ for the low partial waves, but because of the oscillations of f_l and $f_{l'}$, the values it does give tend to have random phase. As a result the small angular momenta do not contribute to the cross section.[26]

Both the adiabatic theory and the distorted waves theory thus are best at forward angles; indeed the Fraunhofer approximation of the adiabatic theory is based on an expansion about $\Theta=0°$. We will now make use of these facts to normalize the distorted waves cross section to the adiabatic cross section at $\Theta=0°$. (By comparing *cross sections* the uncertainties of the individual $I_{ll'}$ are averaged out.) Of course, neither theory should agree well with experiment at $\Theta=0°$, because of the Coulomb excitation which both omit. However, the theories must agree *with each other* at $\Theta=0°$, and a value for V_0 of Eq. (18) which will incorporate this agreement can be obtained.

It is interesting at this stage to derive the 0° amplitude of the adiabatic theory by a method independent of the approximations of Blair and Drozdov. Because the adiabatic amplitude is that part of the elastic scattering amplitude which is first order in the nuclear deformation, we may apply the "optical theorem," which the elastic scattering amplitude must satisfy.[27] According to this theorem

$$\mathrm{Im}f(0°) = (k/4\pi)\sigma_{\mathrm{tot}}, \quad (25)$$

so that the imaginary part of the forward scattering amplitude is related to the total cross section. (Here the amplitude has the usual normalization, such that $|f|^2$ is the elastic scattering cross section, and of course we extrapolate past the region of Rutherford scattering.) Equation (25) shows that if $f(0°)$ were pure imaginary for some simple reason, then $f(0°)$ could be computed simply from σ_{tot}. An estimate of σ_{tot} then would yield an estimate of $f(0°)$. It now shall be argued that this procedure may be followed for "black" nuclei, i.e., for short wavelength particles incident on strongly absorbing nuclei.

For spherical black nuclei the sharp-cutoff approximation for η_l gives $\eta_l=0$ if $l \lesssim l_0$, and $\eta_l=1$ if $l>l_0$. The elastic scattering amplitude and the total cross section are expressed in terms of η_l in the form[17,19,27]

$$f(0°) = (2ik)^{-1}\sum_{l=0}^{\infty}(2l+1)(\eta_l-1),$$

$$\sigma_{\mathrm{tot}} = 2\pi k^{-2}\sum_{l=0}^{\infty}(2l+1)(1-\mathrm{Re}\eta_l).$$

Upon introducing the sharp-cutoff approximation these reduce to

$$f(0°) = -(l_0+1)^2/2ik,$$
$$\sigma_{\mathrm{tot}} = 2\pi k^{-2}(l_0+1)^2.$$

The following observations may be made: (1) The formulas just derived of course verify the optical theorem. (2) They show that the correct total cross section to use in Eq. (24) is that computed in terms of the sharp-cutoff radius, l_0/k. Because the value of this radius is influenced by the Coulomb field, the normalization we derive is automatically Coulomb-corrected. (3) It appears that $f(0°)$ is pure imaginary in this case, so indeed

$$f(0°) = (ik/4\pi)\sigma_{\mathrm{tot}}.$$

When the nucleus is deformed the area it presents to the incident beam is changed, but the total cross section for short wavelengths continues to be twice the area.

[25] It is interesting that for many of the typical values of the imaginary potential the inward-propagating radial wave does not damp to zero at all rapidly, in agreement with McCarthy's graphs. [I. McCarthy, Nuclear Phys. **10**, 583 (1959).] So long as reflection does not occur, however, the nucleus can be "black" to a radial wave if the wave does damp eventually. Igo's discovery that only the surface of U is important is more related to the reflection coefficient at the surface than to any rapid damping of f_l.

[26] Inspection of our calculations indicates that omission of the low partial waves would have some influence in the backward hemisphere, but would cause only minor changes in the forward hemisphere.

[27] L. D. Landau and E. M. Lifshitz, *Quantum Mechanics* (Addison-Wesley Publishing Company, Inc., Reading, Massachusetts, 1958), p. 435; R. J. Glauber in *Lectures in Theoretical Physics* (Interscience Publishers, Inc., New York, 1959), Vol. 1.

Hence, if $f(0°)$ is pure imaginary,

$$f(0°)=(ik/2\pi)\text{ (projected area)}.$$

In Blair's notation[7] the radius of a deformed nucleus in space-fixed coordinates is given as

$$R(\theta_1,\theta_2)=R_0[1+\sum_{l,m}\alpha_{lm}Y_l^m],$$

and up to terms linear in α_{lm} the area may be computed to be:

$$\text{area}=\pi R_0^2[1+2\textstyle\sum_l \alpha_{l0}Y_l^0(\pi/2)].$$

The forward scattered amplitude then becomes

$$f(0°)=ikR_0^2[\tfrac{1}{2}+\textstyle\sum_l \alpha_{l0}Y_l^0(\pi/2)]. \quad (26)$$

Equation (26) agrees exactly with the $\Theta=0°$ limit of Blair's expression, showing the generality of his result.

The $\Theta=0°$ quadrupole cross section is computed by squaring the $l=2$ term of Eq. (26) and averaging over nuclear orientations. For the averaging it is useful to note that $\alpha_{20}=\beta(4\pi/5)^{\frac{1}{2}}Y_2^0(\theta_1,\theta_2)$. It is found that

$$(d\sigma_{fi}/d\Omega)_{0°}=k^2R_0^4\beta^2/16\pi. \quad (27)$$

We now normalize the results of the present paper by choosing the parameter V_0 so that the cross section of Eq. (19) comes out in agreement with the above result.

Probably Eq. (27) should be regarded as a lower bound, since the addition of some real part to the amplitude would increase the 0° cross section. Although the sharp-cutoff approximation does indicate that $f(0°)$ is pure imaginary for spherical black nuclei, it is not clear that the accuracy of that result extends to the small terms that depend on deformation. From Eq. (15) of the distorted waves calculation it is clear that the amplitude which depends on deformation can be imaginary only if the average of $e^{i(\sigma_l+\sigma_{l'})}I_{ll'}$ is imaginary. Some indications to this effect are described in Appendix B. It seems reasonable to define a "black" nucleus as one for which $f(0°)$ is pure imaginary, and to use Eq. (27) as a basis for further computation. In this we agree with other analyses of the adiabatic method.[7,9]

It is noteworthy that the excitation curve of the 0° cross section of Eq. (27) is linear with k^2, a basic scaling law.[7] This is seen to be a special result for black nuclei, a consequence of the constancy of the total cross section. To achieve this result V_0 must vary approximately linearly with E. Values derived for V_0 in Sec. III show such linearity. Some further analysis of energy dependence is given in Appendix B.

The distorted waves method can treat nonzero values for the Q of the reaction ($Q=E_f-E_i$). Unfortunately, the zero degree cross section appears to depend upon Q in a sensitive manner, so interfering with the normalization procedure. To normalize these cases the distorted waves calculation may be repeated with Q set equal to zero, and V_0 determined through Eq. (27). The value so determined for V_0 then can be retained when $Q\neq 0$. This procedure appears proper because the value of Q has more influence upon the manner in which the terms of the l, l' sum combine than upon the values of the individual terms.

III. RESULTS OF COMPUTATIONS

Computations were performed for the inelastic scattering of 20-, 40-, and 60-Mev alpha particles from C, Mg, and Ca, for the case of quadrupole excitation. In these calculations, the effect of the nuclear charge, the smoothing of the wave function and the Q of the reaction were studied independently and in combinations. In addition, we investigated the consequences of employing different smoothing functions. Finally, some cases involving $L=0$, monopole excitation, were computed.

(a) Comparison with Fraunhofer Formula

The distorted waves theory curves which should be most comparable with the Fraunhofer calculations of Drozdov[9] and Blair[7] are those computed without the Coulomb field, and without any smoothing of the wave function (these calculations also omit the Coulomb field, and in the Fraunhofer approximation a sharp-cutoff surface is assumed). For $L=2$ excitation the Blair expression for the angular distribution is proportional to

$$J_0^2(x)+3J_2^2(x), \quad (28)$$

where $x=\rho\Theta$ or $x=2\rho\sin\frac{1}{2}\Theta$. The form of x is uncertain because it depends on a somewhat arbitrary choice of shadow line in applying the Fraunhofer approximation. Figure 1 shows DWB curves for five values of ρ and indicates their comparison with the Blair curves for both choices of shadow line. All curves have been normalized to unity at $\Theta=0°$.

Evidently the agreement is excellent at small angles, as it must be, since at these angles the Fraunhofer approximation is accurate and all choices of shadow line are equivalent. The Fraunhofer approximation is seen to give qualitatively good results even toward much larger angles, although noticeable peak shifts do occur. It appears that neither choice of argument in Eq. (28) is to be preferred over any large interval in angle.

The DWB curves in Fig. 1 show the very interesting feature that the successive peaks are equally spaced in angle, provided regions very near 0° and 180° are ignored. This feature has been noted in some experiments.[28]

The five DWB curves in Fig. 1 are very similar in shape. We note that the peak spacing varies inversely as ρ, a feature which is inherent in the Fraunhofer theories.[7,9] In addition, however, the relative peak heights in the forward angles are nearly identical. This tends to give support to the ideas of "universality" of the diffraction patterns and agrees with Blair's scaling rules.

[28] L. Seidlitz, E. Bleuler, and D. J. Tendam, Phys. Rev. **110**, 682 (1958).

Both the Fraunhofer curves and the DWB curves of Fig. 1 have the property that their envelope falls fairly slowly towards large angles. As additional physical effects come to be considered, the envelope will be seen to fall more rapidly. These effects will now be considered in turn.

(b) The Q of the Reaction

Figure 2 shows the effect of an energy loss of 4.43 Mev for carbon, both with and without the Coulomb field. The calculations were done with sharp-cutoff wave functions and at the convenient energy of 40 Mev. The interaction radius was obtained from the approximate formula

$$R_0=(1.4A^{\frac{1}{3}}+2.0)\text{f}, \tag{29}$$

which is used throughout the present paper, and which agrees well with sharp-cutoff radii used elsewhere.[1,7,29] Then for carbon $R_0=5.21$f. A normalization constant N, obtained by the method described in Sec. II(c) is displayed on the graph.

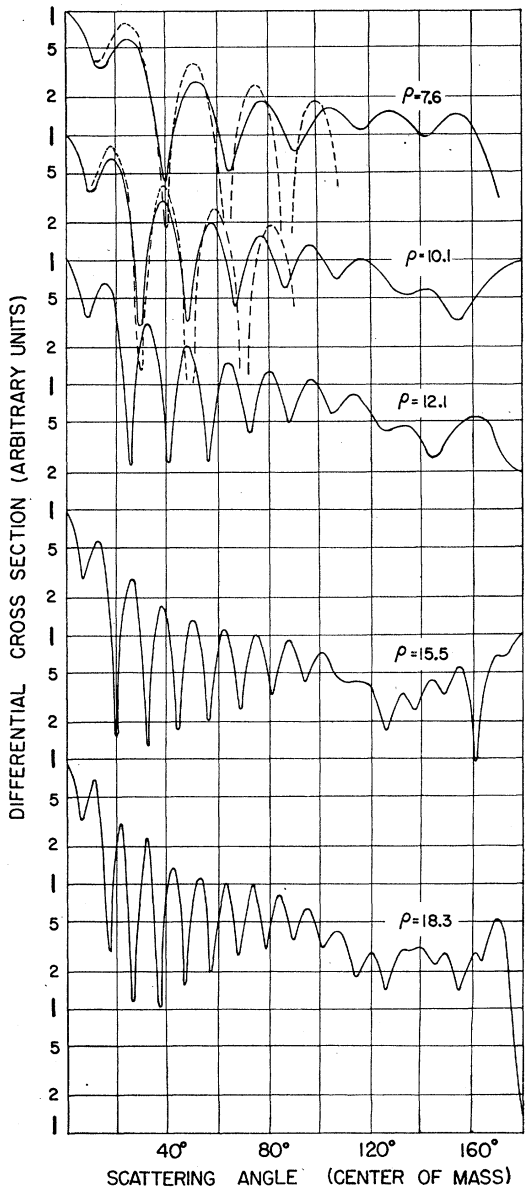

FIG. 1. Angular distributions calculated for several values of $\rho=kR_0$. The Coulomb field is ignored and sharp-cutoff wave functions are employed. The dashed curves give the Blair formula Eq. (28), with argument $\rho\Theta$ for $\rho=7.6$, and $2\rho\sin(\Theta/2)$ for $\rho=10.1$. The curves are normalized to unity at $\Theta=0°$.

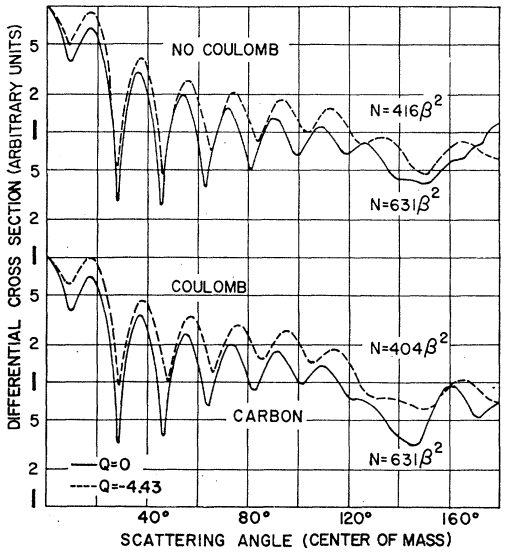

FIG. 2. Angular distributions for $C^{12}(\alpha,\alpha')C^{12*}$ with incident laboratory energy of 40 Mev. Sharp cutoff wave functions are used with $R_0=5.21$f. The effect of energy loss is indicated. All curves are normalized to unity at $\Theta=0°$. The quantity N indicated on the graph is the normalization factor by which the curves should be multiplied to give cross sections in millibarns per steradian.

The primary effect of energy loss enters the calculation in the form of a reduced momentum for the outgoing particle. This, of course, shifts the cross-section pattern to larger angles; however, the general shape of the pattern is not appreciably altered. Inspection of the values of N shows that the heights of the peaks on the two curves also are much the same. Thus it should be quite possible to compensate for the energy loss effect by simple calculation, and not to carry it explicitly.

One of the most important results of the Blair theory[7] is the "phase rule." This rule assigns odd parity to those excitations in which the inelastic angular distributions are in phase with the elastic; it assigns even parity to those in which the cross sections are out of phase. In Fig. 2, the effect of about 10% energy loss is seen to shift the pattern a quarter-cycle, i.e., enough to create doubts in applying the phase rule.

An interesting effect is in evidence near 0°. In this region the cross section can probably be expressed as a function of $q=|\mathbf{k}_i-\mathbf{k}_f|$, with this quantity being used

[29] J. S. Blair, G. W. Farwell, and D. K. McDaniels, Nuclear Phys. **17**, 641 (1960).

in the form qR_0 as the argument in the Fraunhofer formula, Eq. (28). Then if $|\mathbf{k}_i| \neq |\mathbf{k}_f|$ the value of q does not vanish at 0°, and the angular distribution near 0° must be similar to that which would be found at larger angles if $|\mathbf{k}_i| = |\mathbf{k}_f|$ were true. This effect is clearly visible in Fig. 2, and seems to have been observed in a striking way in some (d,d') experiments.[30]

In the remaining calculations we will neglect the Q of the reaction.

(c) Coulomb Field

The effects of the Coulomb field are shown in more detail in Fig. 3, for 40-Mev alpha-particle scattering from C, Mg, and Ca. Unsmoothed wave functions are used. The interaction radius R_0 was chosen as in part (b), and for C, Mg, and Ca, respectively, it has the values 5.21f, 6.04f, and 6.79f.

The Coulomb field causes no very pronounced changes of the angular distributions, in agreement with the idea[7] that the large values of the interaction radius imply a fairly weak effective Coulomb field. Nevertheless, the backward angle cross section is diminished relative to the forward angles, and the peaks of the angular distribution are noticeably shifted toward larger angles. These effects become quite important in the Ca curve.

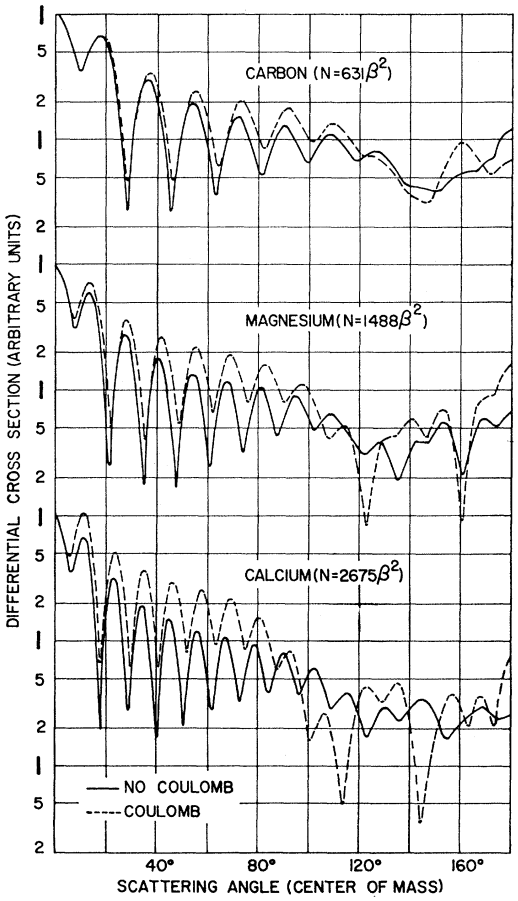

FIG. 3. Angular distributions for C, Mg, and Ca with $R_0=5.21$f, 6.04f, and 6.79f, respectively, at 40 Mev, with $Q=0$. Sharp-cutoff wave functions are used. The effect of the Coulomb field is indicated. The normalization is as described in the caption to Fig. 2.

[30] A. Blair (private communication).

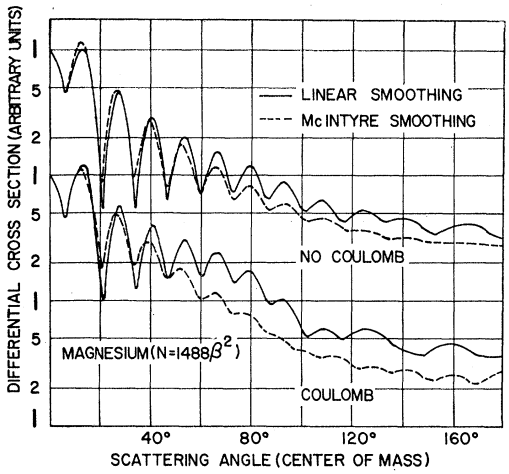

FIG. 4. Angular distributions for $Mg^{24}(\alpha,\alpha')Mg^{24*}$ with incident laboratory energy of 40 Mev, $R_0=6.04$f, and $Q=0$. Linear smoothing, Eq. (22), and McIntyre smoothing, Eq. (21), are presented, with $\Delta l=1.0$ and $\xi^{(0)}=0$. The normalization is as described in the caption to Fig. 2.

The shift of the peaks of the angular distribution would seem to cast doubt on the Blair phase rule, which compares the elastic and inelastic angular distributions. A preliminary study of this question was conducted by comparing the three curves of Sec. IV with the corresponding exact optical-model curves for the elastic scattering. This comparison does agree quite well with the phase rule.

(d) Effect of Smoothing the Wave Function

Two different procedures for smoothing the wave function were employed, as discussed in Sec. II. In one procedure the coefficients of the outgoing amplitudes were varied according to a "Saxon" form factor, as employed by McIntyre.[23] In the other procedure a linear approximation to the McIntyre smoothing was used. Figure 4 compares these two procedures, both with and without the Coulomb field, for the case of 40-Mev alpha particles on Mg. All these curves are much less oscillatory than those computed with nonsmoothed wave functions. Evidently the cross section is quite sensitive to the details of the smoothing, especially in the backward angles. This sensitivity to the smoothing assumptions also is found upon comparing with Fig. 9, for which correct optical-model phase shifts were employed.

Figure 5 shows smoothed curves for C, Mg, and Ca, all at 40 Mev, and all having the same interval of (linear) smoothing. A progressive "tilting" of the curves is apparent. This behavior is very much like that seen in elastic scattering. The similarity bears out in a gratifying way the idea of the *exact* adiabatic method, that the

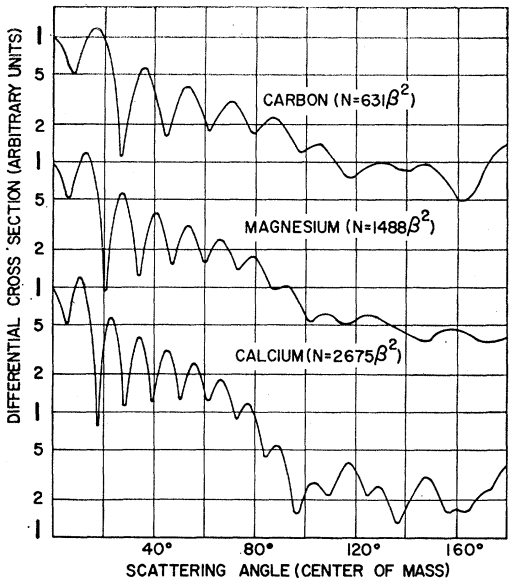

FIG. 5. Angular distributions for C, Mg, and Ca with $R_0=5.21$f, 6.04f, and 6.79f, respectively. Linear smoothing, Eq. (22), is employed with $\Delta l=1.0$ and $\xi^{(0)}=0$ for 40 Mev incident (lab) energy and $Q=0$. The normalization is as described in the caption to Fig. 2.

inelastic cross section is obtained by slight modifications of the elastic cross section.

In several computations a small "nuclear phase shift," i.e., $\xi^{(0)}$ in Eq. (22), was employed with the smoothing function. The effect was noticeable, especially in the vicinity of 90°, but was small relative to the other effects under investigation.

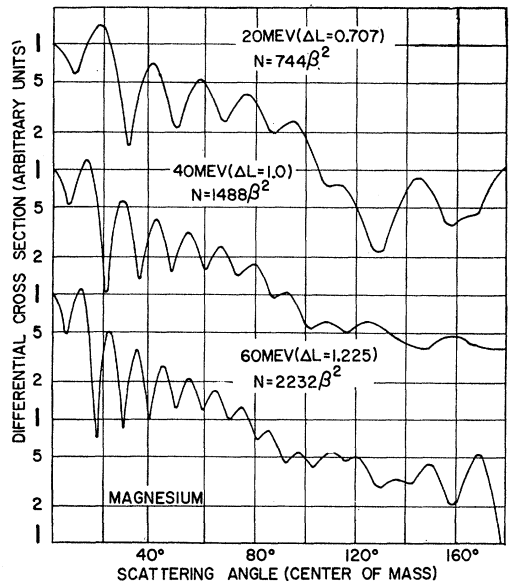

FIG. 6. Angular distribution for $Mg^{24}(\alpha,\alpha')Mg^{24*}$ with $R_0=6.04$f and $Q=0$. Linear smoothing, Eq. (22), is employed with $\xi^{(0)}=0$ and Δl varied in the manner described in Sec. II(b). The normalization is as described in the caption to Fig. 2.

(e) Variation with Energy

Figure 6 shows angular distributions for alpha particles on Mg at incident (laboratory) energies of 20, 40, and 60 Mev. Linear smoothing is employed, as discussed in Sec. II(b). The three curves are very similar in shape. By suitable adjustments of the horizontal and vertical scales they can almost be made to superimpose, in agreement with Blair's scaling laws, and in agreement with a recent tabulation of experimental data.[29] The normalization factor N is given for each curve, and shows the expected linear increase of differential cross section with energy. The parameter V_0 also is expected to vary approximately linearly with energy. It has been extracted, the three values of V_0 being 7.4, 15.2, and 20.1 Mev, respectively, for the 20-, 40-, and 60-Mev cases. These values are reasonable for optical potential strengths at large interaction radii, and are typical of the values of V_0 found for all other cases.

The approximate sharp-cutoff radius introduced in part (b) is independent of energy. Actually R_0 should decrease slightly with energy,[22] and according to a logarithmic law (see Appendix B). The effect is a small one, however and is safely ignored.

(f) Monopole Excitation, $L=0$

For monopole excitation Eq. (19) specializes to

$$(d\sigma/d\Omega)=N'|\sum_l(2l+1)^{\frac{1}{2}}e^{2i\sigma_l}Y_l^0(\Theta,0)f_l(\rho_i)f_l(\rho_f)|^2, \quad (30)$$

where N' is a normalization constant which will not be investigated. It was easy to calculate the monopole cross section with an abbreviated version of the quadrupole program.

Figure 7 shows monopole angular distributions for 40-Mev alpha particles incident on C, Mg, and Ca, using the linear smoothing procedure. Figure 7 is the analog of Fig. 5 for the quadrupole case. The corresponding curves of Figs. 7 and 5 are astonishingly alike, not only in the locations of peaks, but in the detailed structure of the diffraction pattern. This similarity lends support to the phase rule, in that inelastic transitions of the same parity are in phase with each other. The monopole curves agree with the Fraunhofer approximation even better than do the quadrupole curves. This has been displayed in Fig. 7, where $J_0^2(\rho\theta)$ is plotted. The curves virtually coincide for $\theta\lesssim 25°$.

The curves of Figs. 5 and 7 differ somewhat around the 0° peak. The difference probably is not enough to distinguish spins.

IV. COMPARISON TO EXPERIMENT

In this section we compare the results of the distorted waves theory with experimental data. In the calculations the Coulomb field and the energy loss are explicitly taken into account. In addition the smoothing assumptions are replaced by accurate calculations of the

η_l coefficients, as discussed in Sec. II. Three illustrative cases have been chosen, primarily on a basis of availability of data and optical-model potentials. Although we did not attempt to achieve best fits to the data, it will be seen that the agreement with experiment is quite satisfactory. We also did not include Coulomb excitation, so the fits are not expected to be accurate at 0°.

Figure 8 shows experimental and theoretical cross sections for 40-Mev alpha-particle inelastic scattering to the 4.43-Mev (2^+) level of C^{12}. The experimental data is taken from Yavin and Farwell.[1] The theoretical results have been obtained assuming $R_0=5.21$f, as taken from Eq. (29), and have been normalized with $|\beta|\approx 0.4$. The

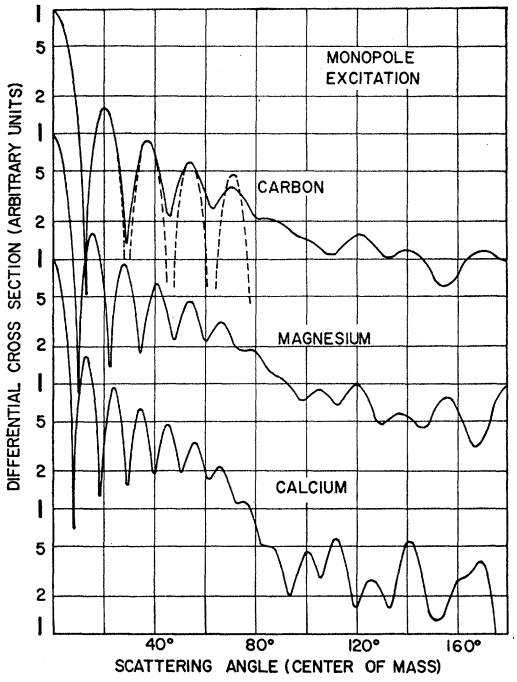

FIG. 7. Angular distributions for monopole excitation as described in Sec. III(f). The radii and smoothing parameters are the same as those described in the caption to Fig. 5. The dashed curve gives the Blair formula, $J_0^2(\rho\Theta)$. All curves are normalized to unity at $\Theta=0°$.

data show little diffraction structure, contrary to predictions of the theory.[31] Part of the disagreement may be due to the breakdown of the "black" assumption. Study of the values of $|\eta_l|$ obtained from optical model calculations[21,32] shows them to be at least as large as 0.1, even for the lowest partial waves. This value is far greater than for the other cases investigated and causes the assumption of Eq. (18) to be more questionable. In this connection it also is helpful to recall that Eq. (27)

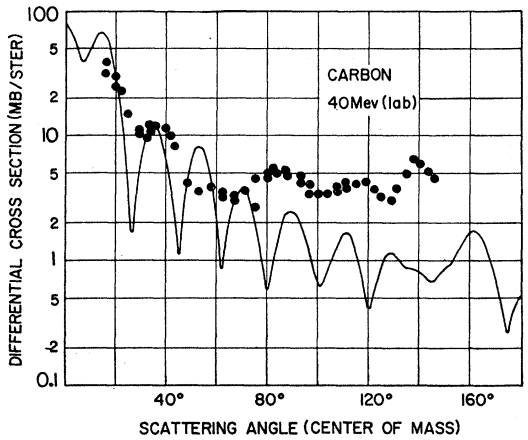

FIG. 8. Angular distributions for $C^{12}(\alpha,\alpha')C^{12*}$ ($Q=-4.43$ Mev) with incident laboratory energy of 40 Mev. Optical-model phase shifts are employed and $R_0=5.21$f. The closed circles denote the experimental cross sections of Yavin and Farwell.[1] The normalization procedure described in Sec. II(c) yields $|\beta|\approx 0.4$.

only is a lower bound to the cross section, a larger cross section being obtained if the forward scattering amplitude has an appreciable real part. It is possible that the apparent large value of $|\beta|$ for carbon is due to the omission of the real part of the forward scattering amplitude in Eq. (27), this being appreciable because the "black" assumption breaks down.

The $Mg^{24}(\alpha,\alpha')Mg^{24*}$ ($Q=-1.37$ Mev) reaction has been extensively studied elsewhere[29] and good agreement with the simple diffraction theory has been found. Hence for this case one should expect to find reasonable agreement between a distorted waves theory and experiment and this is demonstrated in Fig. 9. The 43-Mev angular distribution data of Shook[1] is presented. It has been normalized to the 41-Mev absolute angular distri-

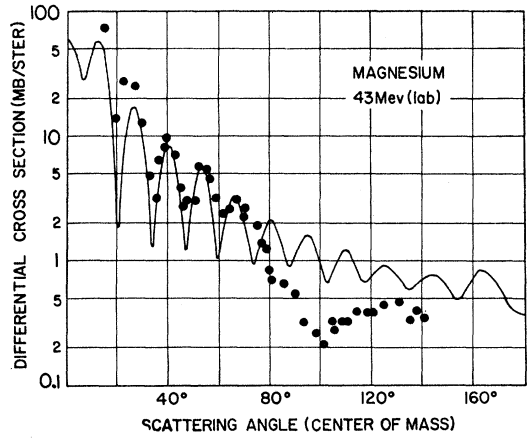

FIG. 9. Angular distributions for $Mg^{24}(\alpha,\alpha')Mg^{24*}$ ($Q=-1.37$ Mev) with incident laboratory energy of 43 Mev. Optical-model phase shifts are employed and $R_0=6.04$f. The closed circles denote the experimental angular distributions of Shook[1] which have been normalized to the 41-Mev absolute angular distribution data of Blair, Farwell, and McDaniels.[29] The normalization procedure described in Sec. II(c) yields $|\beta|=0.20$.

[31] More recent experiments at 28.4, 31.0, and 33.6 Mev do show a pronounced diffraction structure, however. See T. Mikumo, H. Yamaguchi, I. Nonaka, M. Odera, Y. Hashimoto, M. Kondo, and T. Maki, J. Phys. Soc. Japan, **15**, 1158 (1960).

[32] The optical-model parameters were obtained from G. Igo and R. M. Thaler, Phys. Rev. **106**, 126 (1957), for the C^{12} and Mg^{24} cases and from Igo, reference 24, for the A^{40} case.

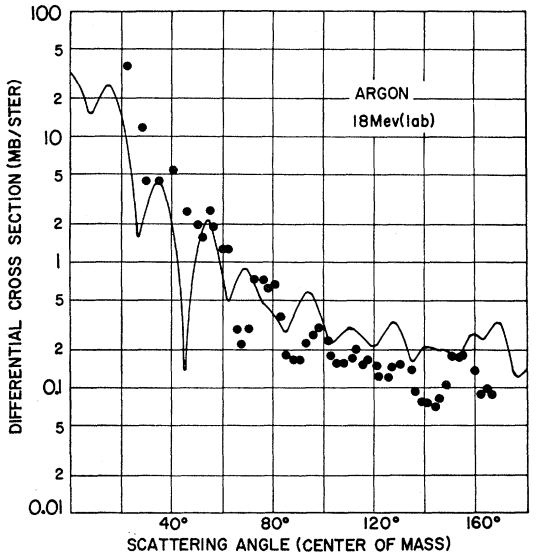

FIG. 10. Angular distributions for $A^{40}(\alpha,\alpha')A^{40*}$ ($Q=-1.46$ Mev) with incident laboratory energy of 18 Mev. Optical model phase shifts are employed and $R_0=6.79$f. The closed circles denote the experimental cross sections of Seidlitz, Bleuler, and Tendam.[28] The normalization procedure described in Sec. II(c) yields $|\beta|\approx 0.1$.

bution data of Blair, Farwell, and McDaniels[29] (the two experiments are in good agreement for the shape of the distribution). Equation (29) yields $R_0=6.04$f for the interaction radius, and the normalization of theory to experiment yields a deformation parameter, $|\beta|=0.20$. This value for $|\beta|$ of course agrees with the value extracted by Blair.

Examination of Fig. 9 indicates excellent agreement between the distorted waves theory and experiment out to about 75°. It is to be noted that the relative heights of the 40°, 53°, and 66° maxima are predicted correctly. The disagreement in the very forward angles may well be due to Coulomb excitation. It is seen that the low magnitude of the backward cross sections is correctly predicted.

The final case to be considered is presented in Fig. 10, which shows differential cross sections for $A^{40}(\alpha,\alpha')A^{40*}$ ($Q=-1.46$ Mev) for 18-Mev alpha particles. The experimental data is taken from Seidlitz, Bleuler, and Tendam.[28] An interaction radius $R_0=6.79$f has been used, as taken from Eq. (29), and in agreement with the detailed studies of the wave function which are reported in Appendix B. A less realistic radius value of 7.5f also was tested, and led to a curve with much less diffraction structure and with a larger cross section in the backward angles. With the curve shown in Fig. 10 a somewhat uncertain value of $|\beta|\approx 0.1$ is obtained from the normalization. Since the A^{40} nucleus is spherical this number certainly is not a deformation parameter. Nevertheless, the argon reaction undoubtedly is a surface reaction, and is interesting because the high Z and low energy imply a large Coulomb distortion.

The agreement between theory and experiment in Fig. 10 is encouraging. Evidently the general trend of the angular distribution is correctly predicted, as is the qualitative shape of the diffraction pattern. The disagreement between experiment and theory in the very forward angles may well be due to Coulomb excitation. This effect could be included in more accurate calculations merely by adding its amplitude to that of the distorted waves theory. The agreement already obtained suggests that a full-scale distorted waves calculation using Eq. (16) might well yield quantitative agreement with experiment even at large angles. Further investigations are planned.

Note added in proof. Further calculations have now been performed. Explicit numerical evaluation of the radial integrals of Eq. (16) gives the cross section of Eq. (17) without any of the further approximations which had to be carried in the present paper. By the use of optical potentials which fit the elastic scattering, an immediate good fit to the inelastic scattering is found, without any additional adjustable parameters. The agreement with experiment found this way is better than in Figs. 8–10. Values used for β parameters are typical of those found in other ways. Coulomb excitation also has been included, and gives some further improvement of the results. Preliminary work with (p,p') reactions also is encouraging.

ACKNOWLEDGMENTS

We wish to thank J. S. Blair and C. A. Levinson for extensive correspondence on the subjects of this paper. We also are grateful to E. U. Baranger, B. L. Cohen, and R. Drisko for several very useful discussions, and to R. Bassel for supplying us with exact optical-model results.

APPENDIX A. GENERATION OF COULOMB WAVE FUNCTIONS

The Coulomb wave functions satisfy the recurrence relations[33]

$$L[(L+1)^2+n^2]^{\frac{1}{2}}\mathcal{Y}_{L+1}=(2L+1)[n+L(L+1)/\rho]\mathcal{Y}_L -(L+1)[L^2+n^2]^{\frac{1}{2}}\mathcal{Y}_{L-1}, \quad \text{(A-1)}$$

where $\mathcal{Y}_L$ denotes either the regular solution F_L, or the irregular solution G_L. The relations can be used[34] to generate Coulomb wave functions from knowledge of the functions for $L=0$ and $L=1$. The method is straightforward for G_L.

For the regular solution, however, Eq. (A-1) is unstable when applied in *increasing* order; it is quite stable though if applied to F_L in *decreasing* order. Indeed in the region $L\gtrsim\rho$, the relative accuracy increases exponentially when F_L is recurred downward in L. Thus we use the approximate asymptotic formula

$$F_L(\rho)\approx\rho^{L+1}/(2L+1)!!, \quad \text{(A-2)}$$

which is valid for $L\gg\rho$. Equation (A-2) is used for the

[33] J. L. Powell, Phys. Rev. **72**, 626 (1947).
[34] I. Stegun and M. Abramowitz, Phys. Rev. **98**, 1851 (1955).

two high values of L and then Eq. (A-1) is applied successively until $L=0$ is reached. The F_0 function is independently calculated in a manner described below and is correctly normalized. The ratio of the normalized F_0 to the F_0 generated by recurrence is then used to renormalize the other F_L functions.

In order to generate the irregular functions, it is necessary to know G_0 and G_1. These may be obtained along with F_0 by using the formulas in Sec. 12 of Fröberg's article.[35] These formulas require the asymptotic inequality $n^2+4n+3<12\rho/5$ (which is easily satisfied in the present work). This method generates Coulomb wave functions which, for the values of L which contribute significantly to the cross section, are accurate to 6 or 7 decimal places.

APPENDIX B. ANALYSIS OF RADIAL INTEGRALS

Two distinct effects cooperate to cause nuclei to behave as black obstacles, and to cause the sharp-cutoff model to be a good first approximation for elastic scattering. Blair has discussed these effects.[22] Briefly, they are: (1) The imaginary part of the optical potential is strong enough so that any partial wave which is not reflected back near the surface is completely absorbed in the nuclear interior. (2) Which partial waves do penetrate past the nuclear surface is determined before the imaginary potential is yet very large, by a competition between the attraction presented by the tail of the optical potential (real part), and the repulsion presented by the centrifugal potential plus the Coulomb potential. Near the classical cutoff the competition is very sensitive to l, and η_l goes rapidly from zero to one as l increases.

The wave function f_l for the lth partial wave may be studied in terms of the "net" real potential for that partial wave,

$$\mathcal{U}_l(r)\equiv\hbar^2 l(l+1)/2Mr^2+ZZ'e^2/r+\mathrm{Re}U(r). \quad \text{(A-3)}$$

In terms of $\mathcal{U}_l$ the Schrödinger equation for f_l is approximately of the form

$$-(\hbar^2/2M)f_l''=[E-\mathcal{U}_l]f_l, \quad \text{(A-4)}$$

inasmuch as $\mathrm{Im}U$ may be neglected for the range of r under discussion. Figure 11 shows $\mathcal{U}_l(r)$ for argon, for a few values of l, using Igo's parameters for the optical potential.[24] The curves are seen to show a pronounced maximum in the region of the nuclear surface. Other ranges of l and other nuclei lead to similar graphs. The maximum of $\mathcal{U}_l$ shifts logarithmically to smaller r as l increases, and tends to disappear altogether for high l. It disappears only if l becomes extremely high, however, and throughout the range of interest of the present

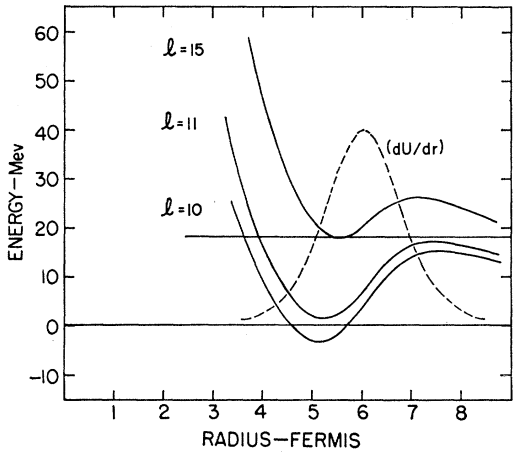

FIG. 11. Sketch of "net" real potential, $\mathcal{U}_l(r)$, for argon as described in Appendix B. The dashed curve shows the variation with radius of the derivative of the real part of the optical potential. The solid horizontal line indicates 18 Mev.

paper all graphs of $\mathcal{U}_l$ look much the same. Evidently for $l\approx l_0$, near the classical cutoff, the height of the maximum nearly equals the total energy, and the maximum is the principal barrier against transmission to the interior. Figure 11 illustrates the case of 18-Mev alpha particles incident on argon, for which $l_0=11.2$. On the whole, waves with $l<l_0$ surmount the barrier, while waves with $l>l_0$ are reflected.

For $l\approx l_0$ the quantity $[E-\mathcal{U}_l]$ in Eq. (A-4) is very small near the maximum of $\mathcal{U}_l$, and the curvature of f_l therefore is small in that region. As a consequence either the real or the imaginary part of f_l grows very large in the region of the maximum of $\mathcal{U}_l$, and this region of r accordingly tends to dominate in the radial integrals $I_{ll'}$. We have evaluated f_{11} numerically for argon at 18 Mev and have found such a maximum. Apparently it is for this reason that the inelastic scattering of alpha particles tends to be a surface reaction. Furthermore, since the maximum of $\mathcal{U}_l$ is located on the outermost tail of the optical potential, the value of V_0 in Eq. (18) must be small, of the order of the values found in Sec. III. It also is clear that V_0 must increase with bombarding energy, because l_0 increases with energy, and the maximum of $\mathcal{U}_l$ shifts to smaller radii as l increases. The optimum value of R_0 in Eq. (18) probably is near the maximum of $\mathcal{U}_l$.

The phase of $I_{ll'}\exp[i(\sigma_l+\sigma_{l'})]$ is of interest in Sec. II(c). This phase is difficult to estimate in any general manner. However, it was found to be very close to 90° for the case of argon at 18 Mev cited above ($l=l'=11$). Such a value was suggested in the text as appropriate for nuclei that are ideally black. Further detailed calculations would show how closely nuclei approach this ideal.

[35] C. E. Fröberg, Revs. Modern Phys. **27**, 399 (1955).